

# Does Morphology Influence Temporal Plasticity?

David C. Sterratt<sup>1</sup> and Arjen van Ooyen<sup>2</sup>

<sup>1</sup> Institute for Adaptive and Neural Computation, Division of Informatics,  
University of Edinburgh, 5 Forrest Hill, Edinburgh EH1 2QL, Scotland, UK  
dcs@anc.ed.ac.uk

<sup>2</sup> Netherlands Institute for Brain Research, Meibergdreef 33, 1105 AZ Amsterdam,  
The Netherlands A.van.Ooyen@nih.knaw.nl

**Abstract.** Applying bounded weight-independent temporal plasticity rule to synapses from independent Poisson firing presynaptic neurons onto a conductance-based integrate-and-fire neuron leads to a bimodal distribution of synaptic strength (Song et al., 2000). We extend this model to investigate the effects of spreading the synapses over the dendritic tree. The results suggest that distal synapses tend to lose out to proximal ones in the competition for synaptic strength. Against expectations, versions of the plasticity rule with a smoother transition between potentiation and depression make little difference to the distribution or lead to all synapses losing.

## 1 Introduction

This paper deals with two phenomena. The first, spike-timing dependent plasticity (STDP), is observed in various preparations (Markram et al., 1997; Bi and Poo, 1998; Abbot and Nelson, 2000). The relative timing of individual pre- and postsynaptic spikes can alter the strength of a synapse (“weight”). The size of the change also depends on the weight, with stronger synapses being depressed more and potentiated less. The second phenomenon is dendritic filtering of synaptic inputs and action potentials. Excitatory postsynaptic potentials (EPSPs) evoked at a synapse are attenuated and spread out temporally on their way to the soma. The dendritic tree also filters backpropagating action potentials (Spruston et al., 1995). The effects of filtering are more pronounced at more distal locations on the dendritic tree.

Theoretical work has suggested that when STDP along with upper and lower bounds on each weight operates at synapses onto a single postsynaptic neuron, the synapses compete with each other to grow strong, leading to a bimodal weight distribution (Song et al., 2000). This model used a conductance-based integrate-and-fire neuron. The aim of this paper is to discover whether the synapse’s location on the dendritic tree affects its ability to change its strength. To do this, we incorporate dendritic filtering and the delay of backpropagating action potentials into the Song et al. (2000) model. A key assumption is that changes to a synapse depend only on signals local to it.

In Sect. 2 we present the neuronal model. In Sect. 3 describe the weight-independent synaptic plasticity rule we use. We look at the behaviour of the rule in Sect. 4. Finally, in Sect. 5, we discuss the implications of this work.

## 2 The Neuron Model

We study a single conductance-based integrate-and-fire neuron with  $N_E$  modifiable excitatory synapses and  $N_I$  non-modifiable inhibitory synapses onto it. Presynaptic spikes are generated according to a Poisson process at a rate  $f_E$  for the excitatory inputs and  $f_I$  for the inhibitory inputs. In this paper  $f_E = 40$  Hz and  $f_I = 10$  Hz.

In order to model the effects of forward and backward filtering, each excitatory input  $i$  is allocated a distance  $x_i$  away from the soma. The distance of each synapse is chosen randomly from a uniform distribution between  $100\mu m$  and  $300\mu m$ . The distance of synapse away from the soma affects the attenuation, delay and time constants of conductance changes evoked at the synapse, as well as the time taken for a backpropagating action potential to reach the synapse from the soma. Inhibitory inputs are assumed to be directly onto the soma.

When a spike arrives at an excitatory synapse there is a delay of  $\Delta^{\text{orth}}(x_i)$  before it increases the conductance  $g_{\text{ex},i}(t)$  in the soma by an amount  $a(x_i)\bar{g}_i$  where  $\bar{g}_i$  is the synapse's maximum conductance (or "weight") and  $a(x_i)$  is a distance-dependent attenuation factor. Inbetween spikes the conductances obey the first-order differential equation

$$\tau_{\text{ex}}(x_i) \frac{dg_{\text{ex},i}}{dt} = -g_{\text{ex},i} \quad (1)$$

where  $\tau_{\text{ex}}(x_i)$  is the time constant of the conductance, which depends on location on the dendritic tree.

Similar equations are obtained for the inhibitory conductances  $g_{\text{in},i}$  except that there are no delays or attenuation factor, the time constant is uniformly  $\tau_{\text{in}}$  and the non-modifiable weights are set to  $\bar{g}_{\text{in}} = 0.05$ .

The membrane potential  $V$  is governed by the update rule

$$\tau_m \frac{dV}{dt} = V_{\text{rest}} - V + \sum_i g_{\text{ex},i}(E_{\text{ex}} - V) + \sum_i g_{\text{in},i}(E_{\text{in}} - V) \quad (2)$$

where  $\tau_m = 20$  ms is the membrane time constant,  $V_{\text{rest}} = -70$  mV is the resting potential,  $E_{\text{ex}} = 0$  mV is the reversal potential of the excitatory synapses and  $E_{\text{in}} = -70$  mV is the reversal potential of the inhibitory synapses. When the membrane reaches a threshold  $\theta = -54$  mV, the neuron fires an action potential and is reset to  $V_{\text{reset}} = -60$  mV.

In order to find how the attenuation factor  $a(x_i)$ , the dendritic delay  $\Delta^{\text{orth}}(x_i)$  and the conductance time constant  $\tau_{\text{ex}}(x_i)$  depend on distance we used the data of Magee and Cook (2000). From their measurement of the relative size of EPSPs at the site of initiation and at the soma, we described the attenuation factor by

$$a(x) = 1 - \frac{x}{375} . \quad (3)$$

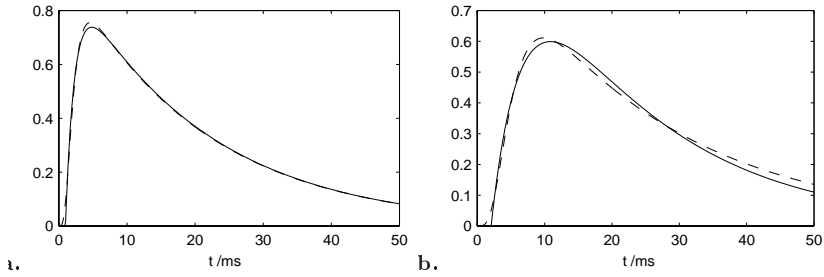


**Fig. 1.** **a.** Fit (solid line) of proximal ( $100\mu\text{m}$ ) EPSP to experimental EPSP (dashed line). Parameters of experimental EPSP were  $\tau_r = 0.5$  ms and  $\tau_d = 20$  ms. Parameters of fit curve were  $\tau = 1.33$  ms,  $\Delta = 0.97$  ms,  $k = 0.96$ ,  $\tau_m = 20$  ms. **b.** Fit of distal ( $300\mu\text{m}$ ) EPSP to experimental EPSP. Parameters of experimental EPSP were  $\tau_r = 2.5$  ms,  $\tau_d = 25$  ms. Parameters of fit curve were  $\tau = 4.62$  ms,  $\Delta = 2.07$  ms,  $k = 1.21$ ,  $\tau_m = 20$  ms.

Magee and Cook (2000) fitted the EPSPs recorded at the soma by the expression  $(1 - \exp(-t/\tau_r))^5 \exp(-t/\tau_d)$  where the rise time  $\tau_r$  and decay time  $\tau_d$  at the soma depend on the distance of the synaptic input along the dendritic tree. In order to incorporate their data into a point neuron model, we used the Levenberg-Marquardt nonlinear regression algorithm (MATHWORKS ftp site) to fit these curves to double-exponential alpha functions of the form

$$k \begin{cases} \left( e^{-\frac{t-\Delta^{\text{orth}}}{\tau_m}} - e^{-\frac{t-\Delta^{\text{orth}}}{\tau_{\text{ex}}}} \right) & t > \Delta^{\text{orth}} \\ 0 & \text{otherwise} \end{cases} \quad (4)$$

where  $k$  is a constant. The decay time constant is identical to the membrane time constant  $\tau_m = 20$  ms of the integrate-and-fire model; this is close to the experimental values. Figure 1 shows the fits for proximal and distal dendritic inputs. We assume that  $\tau_{\text{ex}}(x)$  varies linearly between its endpoint values of  $\tau_{\text{ex}}(100) = 1.33$  ms and  $\tau_{\text{ex}}(300) = 4.62$  ms and that  $\Delta^{\text{orth}}(x)$  varies linearly between its endpoint values of  $\Delta^{\text{orth}}(100) = 0.97$  ms and  $\Delta^{\text{orth}}(300) = 2.07$  ms.

### 3 Synaptic Plasticity

We modified the phenomenological mechanism for the observed plasticity used by Song et al. (2000) so that there was a continuous transition between depression and potentiation at the crossover point. The amount of potentiation or depression depends on signals at the synapse. When a presynaptic spike arrives at the synapse it increases the amount of a substance  $P_i^*$  by  $A_+/\tau_+^*$ . In the absence of spikes, the substance  $P^*$  decays with a time constant  $\tau_+^*$  and catalyses synthesis of a substance  $P_i$ , which in turn decays at a rate  $\tau_+^* = 20$  ms:

$$\tau_+^* \frac{dP_i^*}{dt} = -P_i^* \quad \text{and} \quad \tau_+ \frac{dP_i}{dt} = -P_i + P_i^* \quad . \quad (5)$$

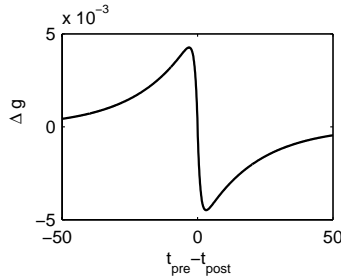


**Fig. 2.** The effective temporal plasticity rule.  $t_{\text{pre}}$  is the time of arrival of the presynaptic spike at the synapse, and  $t_{\text{post}}$  is the time of the backpropagating spike at the synapse. Parameters:  $\tau_+^* = \tau_-^* = 1$  ms,  $A_+ = 0.005$ ,  $A_- = 1.05A_+$ .

When the postsynaptic neuron fires, an action potential starts to backpropagate through the dendritic tree. This backpropagating action potential arrives  $\Delta^{\text{anti}}(x) = x/300$  ms later at the synapse and releases an amount  $A_-/\tau_-^*$  of a substance  $M_i^*$  which decays with a time constant  $\tau_-^*$ . This substance synthesises substance  $M_i$ , which decays at a rate  $\tau_- = 20$  ms. The expression for  $\Delta^{\text{anti}}(x)$  is based on the observation that the propagation speed of the peak of the backpropagating action potential is constant up to about  $300\mu\text{m}$  and that the delay at this point is about 1 ms (Spruston et al., 1995).

The presynaptic spike also decreases the weight by an amount of  $M_i\bar{g}_{\text{max}}$  where  $\bar{g}_{\text{max}}$  is the maximum weight. Similarly, when a backpropagating action potential arrives at the synapse, the weight increases by  $P_i\bar{g}_{\text{max}}$ . The weight is prevented from growing larger than  $\bar{g}_{\text{max}}$  or smaller than zero. The effective temporal plasticity rule is shown in Fig. 2.

In the simulations we set  $A_+ = 0.1$ ,  $A_- = 1.05A_+$  and  $\bar{g}_{\text{max}} = 0.06$ .

## 4 Results

We first ran the model with very small values of  $\tau_+^*$  and  $\tau_-^*$  (0.001 ms) which gave an approximation to the discontinuous case. All simulations lasted 5000 s. After this time the weight distribution was as shown in the top panel of Fig. 3a. This distribution is bimodal; synapses tend to be winners or losers. We can also see that proximal synapses tend to “win” whereas distal ones tend to “lose”.

This result fits with the competitive nature of weight-independent temporal plasticity with bounded weights (Song et al., 2000; van Rossum et al., 2000). Because distal inputs are attenuated, they are less likely to help make the postsynaptic neuron fire and therefore less likely to be potentiated. Temporal factors may also disadvantage distal inputs. Firstly, distal inputs that do help to fire the postsynaptic neuron have to fire earlier than contributing proximal inputs. Secondly, the backpropagating action potential takes longer to reach the distal

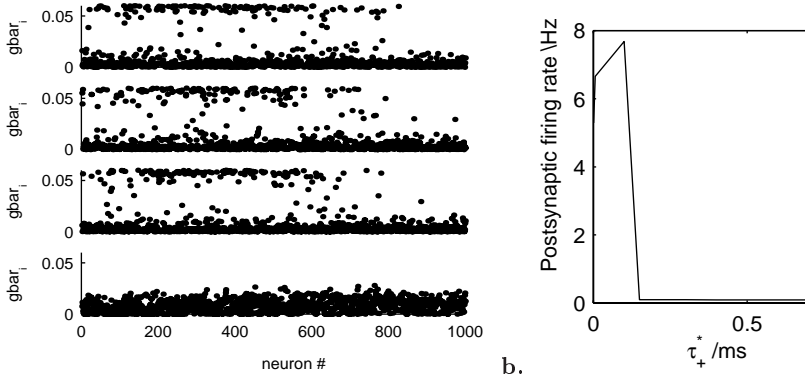


**Fig. 3. a.** The weight distribution for various values of  $\tau_+^*$  and  $\tau_-^*$ . The abscissa of each panel shows the presynaptic neuron number; lower numbers are more proximal and higher numbers more distal. The ordinate shows the strength of the corresponding synapse. From top to bottom the values of  $\tau_+^*$  and  $\tau_-^*$  are 0.001 ms, 0.006 ms, 0.1 ms and 0.15 ms. **b.** The postsynaptic firing rate as a function of  $\tau_+^*$  and  $\tau_-^*$ .

synapses. Thus there is less of the substance  $P_i$  when the backpropagating action potential arrives at distal synapses, and therefore less potentiation.

Could a smoother transition from depression to potentiation alter this behaviour? Bi and Poo's (1998) data shows maximum potentiation and depression peaks separated by  $\pm 5$  ms. If the time of the potentiation peak matches the interval between a contributing presynaptic spike and a backpropagating spike arriving at the synapse, the synapse should be potentiated more.

Figure 3a shows the weight scatter plots for various times of the depression and potentiation peaks. For small values of  $\tau_+^*$  the dependence of the weight distribution on distance does not change much, though a shorter transition phase seems to favour distal synapses. For  $\tau_+^* > 0.15$  ms, all the weights lose, contrary to our hypothesis that smoother curves should favour distal synapses.

The behaviour with higher values of  $\tau_+^*$  is presumably because the peaks of the plasticity curve overlap with presynaptic spikes that are uncorrelated to the postsynaptic spikes, and depression is stronger than potentiation. This idea is confirmed by the dependence of firing rate on the width of the central section (Fig. 3b) which shows that the firing rate of the neuron is around 6 Hz and 8 Hz for smaller values of  $\tau_+^*$  but almost zero for larger ones.

## 5 Discussion and Conclusions

In short, morphology does influence temporal plasticity — at least with the neuron model, temporal plasticity rule and input firing statistics we used. In this section we discuss these caveats.

Our point neuron model with morphology modelled by location-dependent delays and EPSP rise time constants could not include factors that could be modelled using compartmental models, such as dendritic conductances, branching and dendritic width. Although this does limit the scope of the conclusions, we believe that the simpler model gives a first-order understanding of the problem.

Different firing statistics, for example temporally-correlated inputs, affect the weight distribution in pure point neuron models (Song et al., 2000; van Rossum et al., 2000). It seems unlikely that they could affect our results, unless the correlated inputs occurred preferentially over the distal dendritic tree, and were therefore more effective than proximal correlated inputs. Also, successful synapses hit the same upper bound regardless of their location.

The weight-dependent rule studied by van Rossum et al. (2000) leads to a unimodal weight distribution in which synapses cluster around the weight at which depression becomes more potent than potentiation. Temporal properties are much less important, so in our model we would not expect the synaptic weights to depend on location. Preliminary simulations bear out this hypothesis.

A uniform weight distribution leads to distal inputs being less effective. Magee and Cook (2000) have shown that distal synapses in CA1 pyramidal neurons compensate for dendritic filtering by being stronger. Neither weight-dependent nor weight-independent rules appear to lead to this weight distribution. A location-dependent plasticity rule might account for location-dependent weights. Further work will investigate location-dependent plasticity rules derived from synapse-local signals in compartmental models (Rao and Sejnowski, 2001).

## References

1. Abbott, L. F., Nelson, S. B.: Synaptic plasticity: taming the beast. *Nature Neuroscience* **3** (2000) 1178–1183
2. Bi, G.-q., Poo, M.-m.: Synaptic modifications in cultured hippocampal neurons: Dependence on spike timing, synaptic strength, and postsynaptic cell type. *Journal of Neuroscience* **18** (1998) 10464–10472
3. Magee, J. C., Cook, E. P.: Somatic EPSP amplitude is independent of synapse location in hippocampal pyramidal neurons. *Nature Neuroscience* **3** (2000) 895–903
4. Markram, H., Lübke, J., Frotscher, M., Sakmann, B.: Regulation of synaptic efficiency by coincidence of postsynaptic APs and EPSPs. *Science* **275** (1997) 213–215
5. Rao, R. P. N., Sejnowski, T. J.: Spike-timing-dependent Hebbian plasticity as temporal difference learning. *Neural Computation* **13** (2001) 2221–2237
6. Song, S., Miller, K. D., Abbott, L. F.: Competitive Hebbian learning through spike-timing-dependent synaptic plasticity. *Nature Neuroscience* **3** (2000) 919–926
7. Spruston, N., Schiller, Y., Stuart, G., Sakmann, B.: Activity-dependent action potential invasion and Calcium influx into hippocampal CA1 dendrites. *Science* **268** (1995) 297–300
8. van Rossum, M. C. W., Bi, G. Q., Turrigiano, G. G.: Stable Hebbian learning from spike timing-dependent plasticity. *Journal of Neuroscience* **20** (2000) 8812–8821